JOURNAL OF COMPUTATIONAL PHYSICS **124,** 162–176 (1996)
ARTICLE NO. 0051

Stability of Explicit Schemes in the Physical and Frequency Domains

SAMPATH PALANISWAMY AND SUKUMAR R. CHAKRAVARTHY

Computational Fluid Dynamics Department, Rockwell Science Center, Thousand Oaks, California 91360

Received June 8, 1994; revised June 13, 1995

We look at some of the issues involved in designing stable explicit numerical schemes for linear advection equations from two perspectives: (a) in the physical domain, where each scheme represents a particular interpolation of discrete data, and (b) in the frequency domain, where the behavior of each scheme is determined by the spectral characteristics of the operator that is acting on discrete data. We show that (1) the fully discrete form is equivalent to choosing a value for the dependent variable from an interpolation of the data in the spatial domain at the previous time level, (2) interpolation generates a continuous function (polynomial) in the physical space, (3) size of the time step used in updating the solution determines the location from where the interpolated value is obtained, and (4) if a choice of step size shows amplification in the spectral domain, interpolation in the physical domain exceeds the bounds set by the discrete data at a spatial location corresponding to this step size. Comparisons are made between the behavior of the operator in the frequency and physical domains; and the amplification in the frequency domain matches the value of extrema generated by the interpolation. Examples to illustrate both perspectives include first and second difference operators, spatial averaging, and various central and upwind schemes for the linear advection equation.

INTRODUCTION

A scalar advection equation with initial values specified along x, $0 \le x \le L$, is written as

$$\frac{\partial u}{\partial t} + \mathbf{a}\frac{\partial u}{\partial x} = 0,$$

where $u(x, t = 0) = u_0(x)$ is the initial value. We need to specify appropriate boundary conditions at $x = 0$ or L, depending on the sign of $\mathbf{a}$.

When the spatial operator is discretized, the advection equation becomes a system of linear equations. This is the semidiscrete form (time continuous) of the advection equation.

$$\frac{\partial}{\partial t}\overline{U} = \mathbf{a}A\overline{U},$$

where $\overline{U}(t)$, an N vector is the spatial discretization of u, and A is a $N \times N$ matrix whose nonzero entries form a narrow band around the diagonal. Boundary conditions specified at $x = 0$ and $x = L$ also affect the eigenvalue spectrum of A.

The fully discrete form of the equation is obtained on discretizing the temporal behavior. At time level $n + 1$, U is expressed as

$$U^{n+1} = B(U^n),$$

where U_j^n is the jth component of U at time level n.

The design of a numerical scheme should take into account consistency, stability, and convergence characteristics of the implementation. In the limit of temporal and spatial steps, Δt and Δx, approaching zero, consistency means that the fully discrete form of the equation approaches the differential equation. Expanding the fully discrete equation in a Taylors series in time and space and subtracting from the exact differential equation gives the error in terms of the step sizes Δt and Δx. These remainder terms show the limiting behavior of the discrete equation as the mesh sizes shrink. The rate at which a consistent scheme approaches the differential equation determines the order of accuracy of the scheme.

Having discretized the equation, stability determines whether the solution remains bounded. From the semidiscrete form of the equation we can determine if the numerical solution will remain bounded for all time. Eigenvalues of the spatial operator A determine the boundedness of the solution. The next step is to discretize in time and advance the solution to the next time level. This step causes the scheme to become fully discrete and raises the possibility that the solution might not remain bounded for any or all values of the time step Δt, even though the semidiscrete form has a bounded solution for all time $t > 0$. Eigenvalues of B that determine the boundedness of the numerical scheme depend on Δt. Such schemes are known as conditionally stable schemes, and the time step value of Δt for which the fully discrete form has growing solutions deter-

0021-9991/96 $18.00

mines the stability limit for the scheme. The stability limit is a bound on Δt within which the fully discrete form of the equation also has stable solutions for all time. The stability limit is usually presented as an upper bound on the size of the time step. However, as we show later, schemes such as the one based on one-sided four point cubic interpolation remain stable only for $1 \leq \lambda \leq 2$ ($\lambda = \mathbf{a}\Delta t/\Delta x$). Hence stability is more appropriately thought of in terms of both an upper and a lower bound for Δt for a given Δx.

Convergence is a measure of the limiting behavior of the numerical solution to the discrete equation. A numerical solution is said to converge if it can be made to approach, as closely as desired, the exact solution to the differential equation by shrinking the sizes of the temporal and spatial discretizations. For well-posed problems, consistency and stability imply convergence [1].

INTERPOLATION AND STABILITY

Usually the fully discrete form of the scheme is interpreted as expressing U at the new time level in terms of the discrete values of U at previous time levels. It does involve an intermediate step, a map from R^m to R^∞ (from discrete to a continuous function space) executed at each of the j that make up the spatial discretization; m is the number of discrete values U_j^n used in updating the value U_j^{n+1}. Values in the function space generated by this mapping are not bounded by the values in R^m unless the entries of the rows of B satisfy this restriction. If new global extrema are generated in the function space, it can be translated back to the discrete space R^n at the new time level $n + 1$, depending on the location from where the value is chosen to update the solution. This in turn depends on the size of the time step Δt. Stability of numerical schemes for the advection equation can therefore be viewed as a requirement that the underlying interpolation should not generate new upper or lower bounds for the discrete values of U for every frequency resolved by the grid. When a scheme is said to be unconditionally stable, it means that extrema in the function space are bounded for all values of time step Δt. A scheme is conditionally stable if a $\tau_1 < \Delta t < \tau_2$ can be chosen so that the extrema generated in the function space is not translated to R^n at the new time level $n + 1$.

A scheme is said to have a perfect-shift property if for certain specific values of λ, the entries of U^{n+1} are obtained by shifting the elements of vector U^n to the right by an appropriate amount. This is equivalent to passing the vector through a system with a time-delay. In this case, the interpolation step from R^m to R^∞ is eliminated and stability is not an issue.

STABILITY ANALYSIS

Assuming that the semidiscrete form has bounded solutions (spatial discretization does not generate positive eigenvalues for A), we can look at the fully discrete form to assess the stability limits of the difference equations. For linear problems, on an infinite domain or on a finite domain with periodic boundary conditions, the Von Neumann method of stability analysis is often used. In this method, stability is determined by examining the amplitude of input harmonics [1]. The stability bound is defined as a contour in the complex plane which determines the size of the time step Δt (or λ). One could also use the Matrix method [2], where the norm of the operator B determines stability. The advantage of the matrix method is that it includes the effect of boundary conditions in the analysis. Furthermore, this method can be employed even on discretizations over nonuniform meshes. When the fully discrete operator is symmetric, stability is assured whenever the eigenvalue spectrum of the operator is contained within the unit circle [3]. For nonsymmetric operators frequently encountered in advection problems, the solution remains bounded at large times if the eigenvalue spectrum is contained in the unit circle, but it can grow in amplitude for short times. For the solution not to have growth (in the L_2 norm) after each invocation of the operator, the correct measure is the matrix norm, or, equivalently, the operator $(B^{\mathrm{T}}B - I)$ must be negative definite [4].

SPECTRAL CHARACTERISTICS OF OPERATORS

In the Von Neumann method, one compares the amplitude and phase of input harmonic signals after it is acted on by the difference scheme. The result of the analysis is a set of eigenvalues corresponding to eigenvectors that are harmonics of different frequencies on the grid. The magnitude of the eigenvalues determines the amplification and the imaginary part provides the phase shift in the frequency domain or advection in the physical domain. This is equivalent to studying the operator in the frequency domain.

Linear operations like differentiation, averaging, advection with a constant velocity, etc. can be viewed as convolutions of input data with a response function. For the discrete case, the matrix representation of these operators has constants along its diagonals and is known as a Toeplitz matrix or a convolution matrix. The result of these linear operations is, in the frequency domain, the product of the response function and the input data [5]. In studying the operators in the frequency domain we use the Fourier transform to estimate magnification as well as the phase shift imposed on the input data.

The frequency domain of the response function gives

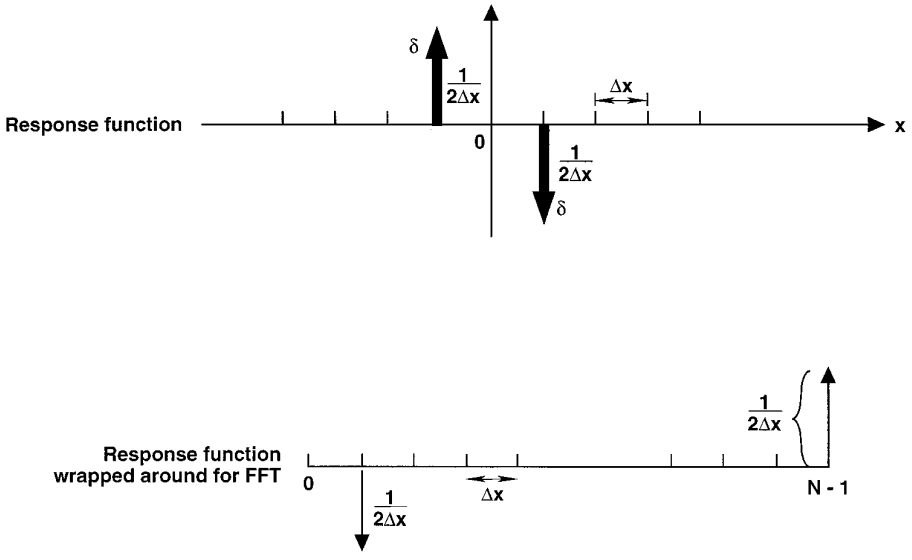

FIG. 1. First difference operator (three-point central stencil).

the amplification, as well as the phase shift of the convolved signal over the frequency range $(-f_n, +f_n)$ (Nyquist frequency $f_n = 1/2\ \Delta x$). When the fully discrete form of the partial differential equation is cast as a response function, the stability bounds on the time step size can be obtained as the domain of Δt that does not generate amplification greater than one for all frequencies resolved by the discretization. For discrete data the response function is an aggregate of delta functions. The Fourier transform of a delta function located at $j + 1$ is $e^{i2\pi f \Delta x}$. The sum of these delta functions make up the representation of the operator in the frequency domain. The amplitude and phase response can be evaluated directly, but we use FFT which is more efficient in generating this information. One call to a FFT [6] routine generates amplitude and phase information over the entire frequency range for a particular step size Δt.

Treating operations as convolutions provides better insight into the effect of these operations on discrete data. This approach can be used to evaluate stability bounds when selecting numerical schemes for differential equations or in choosing appropriate stencils for evaluating derivatives and in designing various smoothing functions. To demonstrate the advantage of viewing the linear operations as convolution, we first look at the frequency

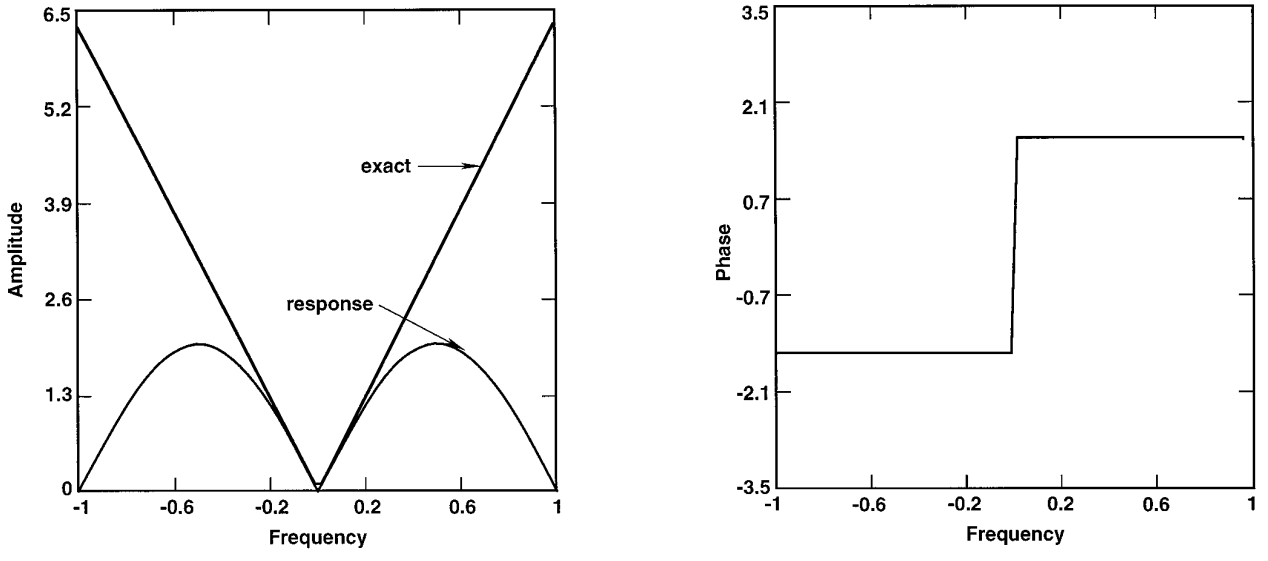

FIG. 2. (a) Amplitude response of three-point central stencil. (b) Phase response of three-point central stencil.

domain of some of the widely used spatial operators like the first difference operator, the second difference operator, and the spatial averaging operator. Central difference operators have a poor amplitude response to high frequency signals when estimating slopes. Upwinded operators have better amplitude response, but phase errors are large at higher frequencies. Second derivatives are best represented by unbiased stencils, although amplitude errors at higher frequencies are large. The frequency domain of the spatial averaging operator shows an interesting behavior. Simple averaging does not rid the data of the highest frequency component. It does, however, squash the component that belongs to one-half of the Nyquist frequency. To remove high frequency data, left- or right-biased averaging or their combination is more suitable. Following this, several numerical schemes for solving the advection equation are presented, along with their characterization in the frequency and physical domains.

FIRST DIFFERENCE OPERATORS

In the discrete form, a delta function is approximated by a square pulse of height $1/\Delta x$ and width Δx, centered at one of the locations from 0 to $N-1$ sample points that make up the data space. The range of frequencies over which amplitude and phase data can be obtained depends on the Nyquist frequency $1/2\ \Delta x$, where Δx is the sampling interval (or step size of the spatial discretization) with a frequency resolution of $1/N\Delta x$. A second-order accurate central difference operator for the first derivative at spatial location j is given by

$$\frac{U_{j+1} - U_{j-1}}{2\,\Delta x}$$

whose frequency domain representation is

$$i\frac{\sin(2\pi f \Delta x)}{\Delta x}\, e^{i2\pi f j \Delta x}$$

with eigenvalue $i\ (\sin(2\pi f\ \Delta x)/\Delta x)$.

The corresponding response function is a delta function centered at $j = 2$, multiplied by a scalar $-1/2\ \Delta x$ and another delta function at $j = N$ multiplied by $+1/2\ \Delta x$ as shown in Fig. 1.

Spectral characteristics of this operator from a discrete FFT output are shown in Figs. 2a and 2b. In the differential form, the first derivative operator should have a magnitude of $2\pi f$ and a phase of $+\pi/2$ for $f > 0$ and $-\pi/2$ for $f < 0$. The second-order accurate central difference operator does not have any phase error throughout the frequency range that can be resolved on the grid, but the magnitudes at higher frequencies are far from the exact value. The magnitude behaves as $\sin(2\pi f \Delta x)/\Delta x$ for $-f_n \le f \le f_n$. To maintain an accurate estimate of the derivative, wave numbers (wave number of one corresponds to frequency f_n) must be restricted to less than about a fifth. This works out to having about 15 points per wavelength for the highest frequency contained in the discretized signal.

Compared to this, the magnitude variation for a one-sided difference operator,

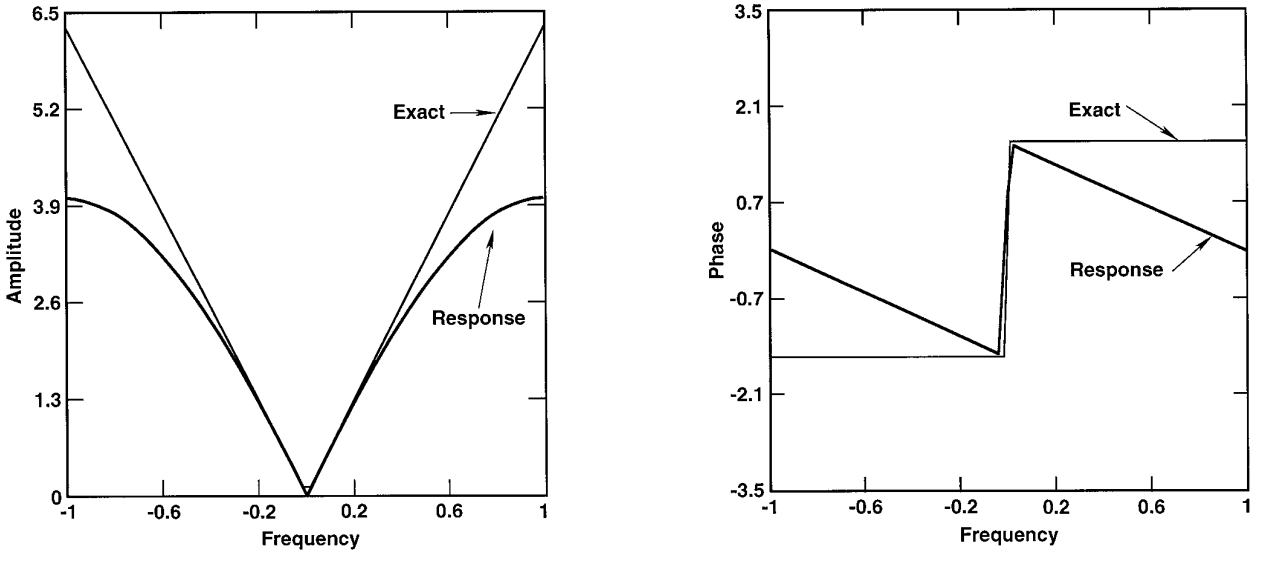

FIG. 3. (a) Amplitude response of two-point upwind stencil. (b) Phase response of two-point upwind stencil.

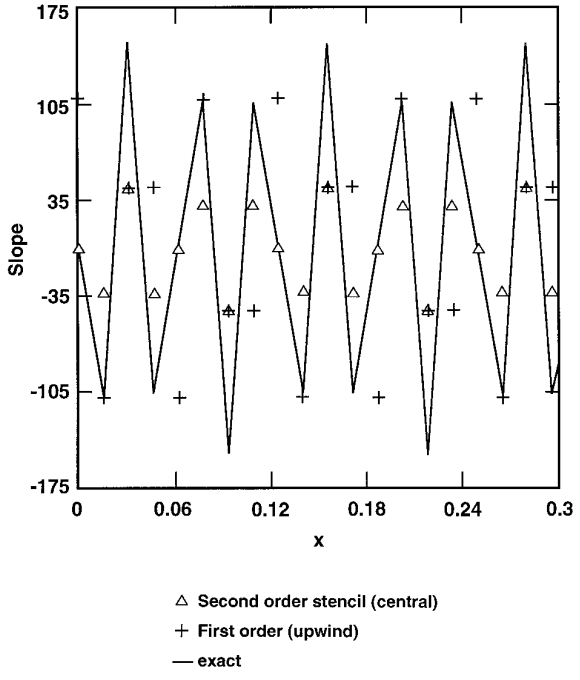

FIG. 4. First derivative in the physical domain.

$$\frac{U_j - U_{j-1}}{\Delta x}$$

(Fig. 3a), is more promising. The spectral representation is

$$\frac{1 - \cos(2\pi f \Delta x)}{\Delta x} + i\frac{\sin(2\pi f \Delta x)}{\Delta x}.$$

At the maximum frequency, the amplification is $2/\Delta x$ instead of $\pi/\Delta x$. However, a look at the phase variation (Fig. 3c) shows that phase error varies from $-\pi/2$ to $+\pi/2$ for frequencies $-f_n$ to $+f_n$. Although the one-sided or upwinded difference operator has better magnitude estimates the phase error is nonzero at almost all frequencies. The result is that, on reconstruction in the physical domain, large errors are inevitable in estimating the location of maximal and minimal slopes. The central difference operator does not suffer from this, although the amplitude estimates are dismal. Figure 4 shows the actual and estimated slopes from the central and one-sided difference operators for a signal with wave number 0.75. In a scenario where estimates for the magnitude of gradients and not the exact location of these maxima are needed, the one-sided operator can do much better than the central difference operator of higher order accuracy.

The spectrum of five-point central difference operator

$$\frac{-U_{j+2} + 8U_{j+1} - 8U_{j-1} + U_{j-2}}{12\,\Delta x}$$

given by

$$i\left[\frac{-\sin(4\pi f \Delta x)}{6\,\Delta x} + \frac{4\sin(2\pi f \Delta x)}{3\,\Delta x}\right]$$

shows that the magnitude estimates are better up to a frequency of roughly $\frac{1}{3}$ of f_n (Fig. 5a). This would mean that for accurate estimates, at least nine points are needed per wavelength at the highest frequency. The magnitude at higher frequencies are between that of the three-point operator and the one-sided operator. At higher frequencies, magnitude drops off rapidly.

The seven-point central difference operator

$$\frac{U_{j+3} - 9U_{j+2} + 45U_{j+1} - 45U_{j-1} + 9U_{j-2} - U_{j-3}}{60\,\Delta x}$$

which reduces to

$$i\left[\frac{\sin(6\pi f \Delta x)}{30\,\Delta x} - \frac{9\sin(4\pi f \Delta x)}{30\,\Delta x} + \frac{3\sin(2\pi f \Delta x)}{2\,\Delta x}\right]$$

in the frequency domain still does not provide better estimates as can be seen from the spectrum at higher wave numbers (Fig. 5a), although the footprint of the stencil is three points wide on either side of the point at which it is applied. This stencil cannot be applied near boundaries where either a three-point stencil or one-sided differences may have to be employed. The amplitude estimates are accurate up to about $\frac{1}{2}$ of f_n. Central difference operators do not introduce phase errors over the entire frequency range (Fig. 5b).

Shifting the stencil to the left results in a upwind biased stencil spanning $j - 2$ to $j + 1$,

$$\frac{2U_{j+1} + 3U_j - 6U_{j-1} + U_{j-2}}{6\,\Delta x}$$

with a spectral representation given by

$$\frac{3 - 4\cos(2\pi f \Delta x) + \cos(4\pi f \Delta x)}{6\,\Delta x} + i\left[\frac{8\sin(2\,\pi f \Delta x) - \sin(4\pi f \Delta x)}{6\,\Delta x}\right]$$

does better than the seven-point stencil (Fig. 6a) in estimat-

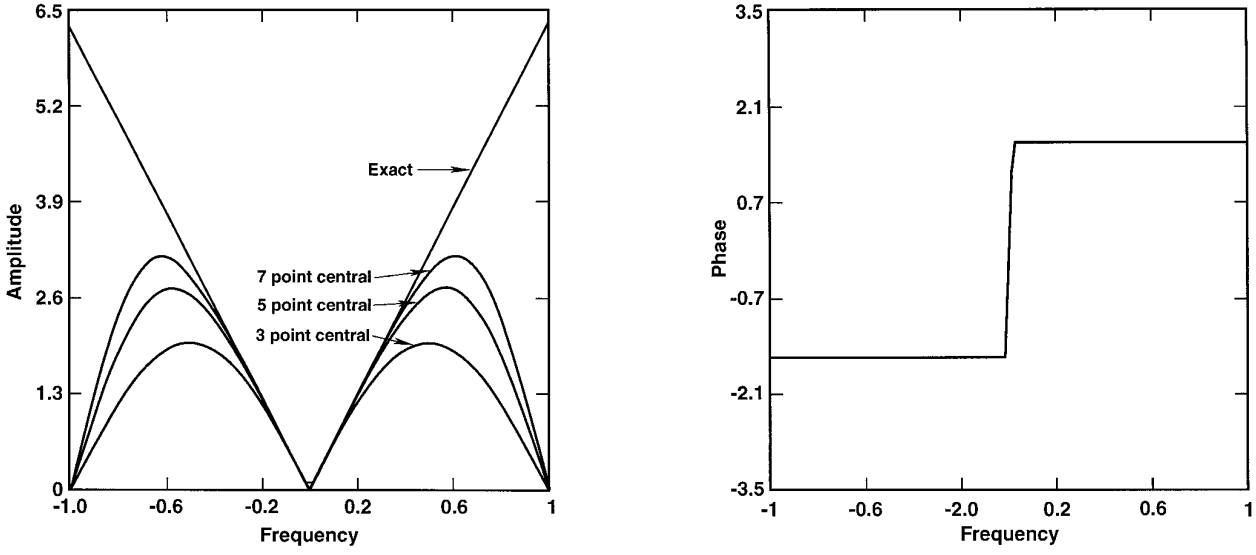

FIG. 5. Frequency domain of central stencils: (a) amplitude response; (b) phase response.

ing the magnitude at higher wave numbers and its phase error is less than that of the first-order accurate two-point upwind stencil (Fig. 6b).

SECOND DIFFERENCE OPERATORS

The exact eigenvalue for the second derivative is $(2\pi f)^2$, is real with a maximum of $(\pi/\Delta x)^2$ at the Nyquist frequency. A three-point central difference operator estimates the magnitude reasonably accurately up to a wave number of little less than a half of the maximum wave number (Fig. 7a). Again the central differenced operator does not introduce phase error. The eigenvalue spectrum for the three-point central differenced operator is

$$\frac{abs(2\cos(2\pi f\,\Delta x) - 2)}{\Delta x^2}$$

with f ranging from $-f_n$ to $+f_n$. At the Nyquist frequency the estimate for the amplitude is $2^2/\Delta x^2$ instead of $\pi^2/\Delta x^2$. When a five-point stencil is used, as can be seen in the

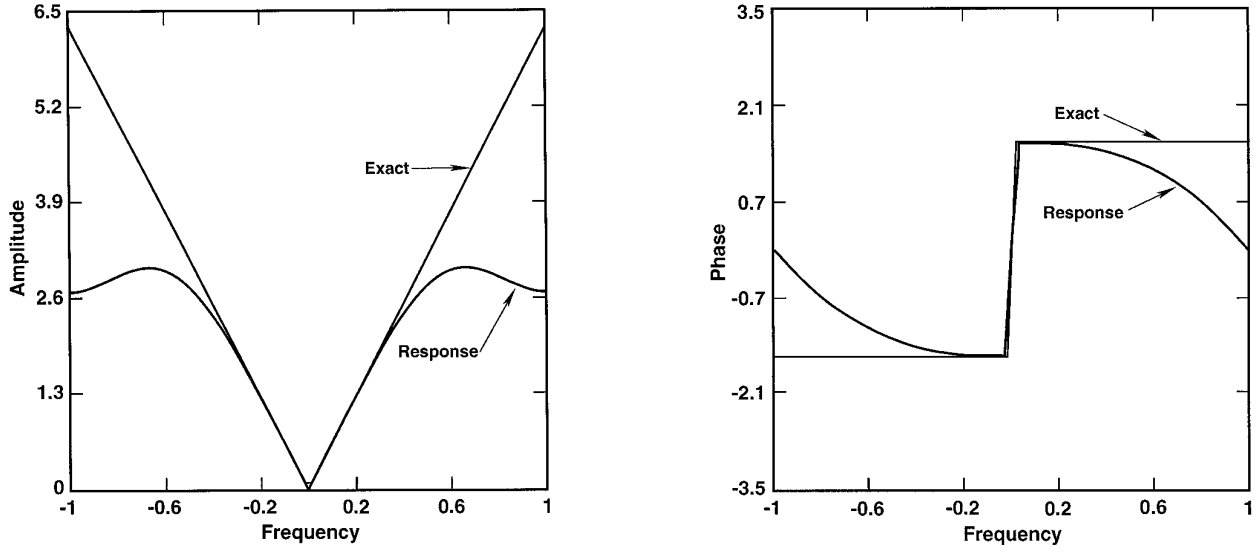

FIG. 6. (a) Amplitude response of upwind biased stencil. (b) Phase response of upwind biased stencil.

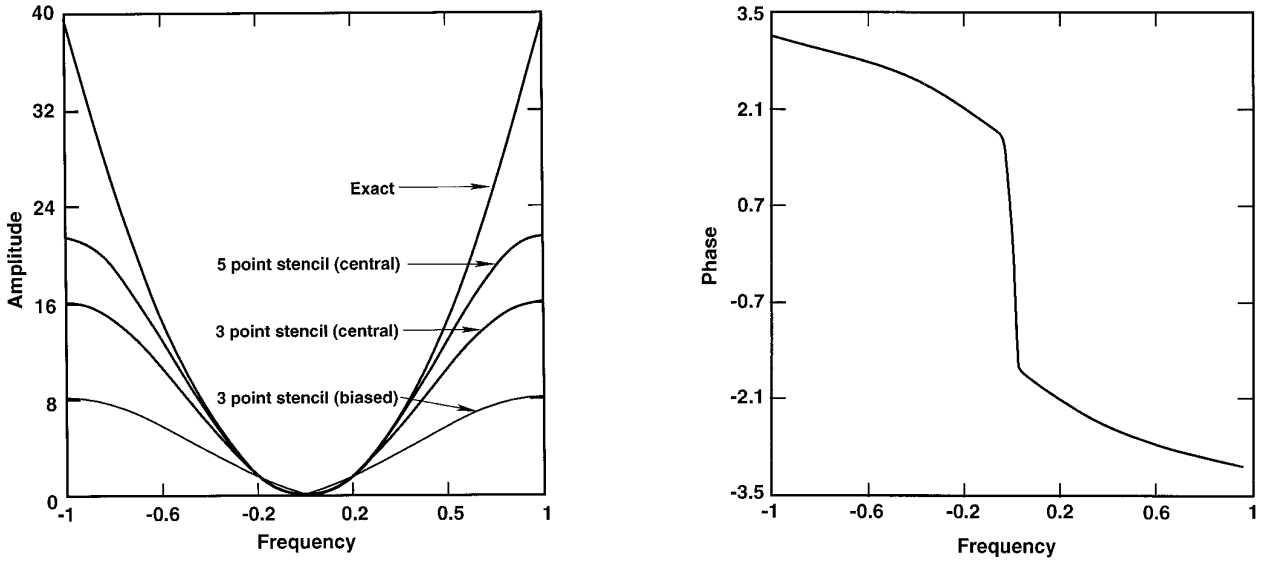

FIG. 7. (a) Frequency domain of second difference operators (amplitude). (b) Phase response of second difference operator (upwind biased).

Fig. 7a, amplitude estimates improve but still are lacking at higher wave numbers. Biased stencils have poor amplitude response when used to evaluate the second derivative. Figure 7a shows the amplitude response for a three-point stencil weighted to the left. Furthermore, biased stencils also introduce phase errors (Fig. 7b). Attempting to fit a cubic polynomial from $j + 1$ to $j - 2$ also leads to the three-point central stencil for the second derivative at j.

Solutions to Navier–Stokes equations require estimates for second derivatives to evaluate the viscous transport terms. As seen from the response curves of the difference operators, since the amplitudes at high frequency are lower than their exact value, the decay rate of the high frequency will also be lower than their actual value. In other words, high frequency is being acted on by a lower viscosity than the low frequency components. This is similar to pseudoplastic behavior common in the flow of plastics.

SPATIAL AVERAGING

Amplitude response of unbiased spatial averaging is shown in Fig. 8a. Smoothing is accomplished by

$$\frac{U_{j+1} + U_{j-1}}{2}.$$

Loss of high frequency information would be expected by averaging the data. Figure 8a shows that the high frequency information is not damped by averaging, although a phase error is introduced into the data by the averaging process. Figure 8b shows that data containing the high frequency component is phase shifted by π. In fact, signals at one-half of the Nyquist frequency are damped out completely, while data containing frequency close to this frequency are damped to varying degrees (Fig. 8a). When a left- or right-biased stencil or a combination of both is used as an averaging operator, the amplitude response is similar to that of a low-pass filter. It damps out the high frequency components of the data (Fig. 8c). Biased averaging introduces phase shifts that vary linearly from 0 to $\pm\pi/2$ at the Nyquist frequency, depending on whether the right- or left-biased stencil is used in the operator (Fig. 8d).

DISCRETIZATIONS FOR THE ADVECTION EQUATION

Let us look at a single hyperbolic partial differential equation with initial condition and for convenience let the boundary conditionis in x be periodic. Solutions $u(x, t)$ for $t > 0$ is of interest, and we want to construct numerical schemes to update the solution U at a discrete set of points from time t to a new time $t + \Delta t$.

For brevity, superscript n is omitted and U_j is used to represent U_j^n. Fitting a straight line in space between points $j - 1$ and j for $\tilde{U}(x)$ results in

$$\tilde{U}(x) = U_j + \left[\frac{U_j - U_{j-1}}{x_j - x_{j-1}}\right] x,$$

a linear interpolation in space. Here the map takes R^2 to the continuous function space. To advance the solution at

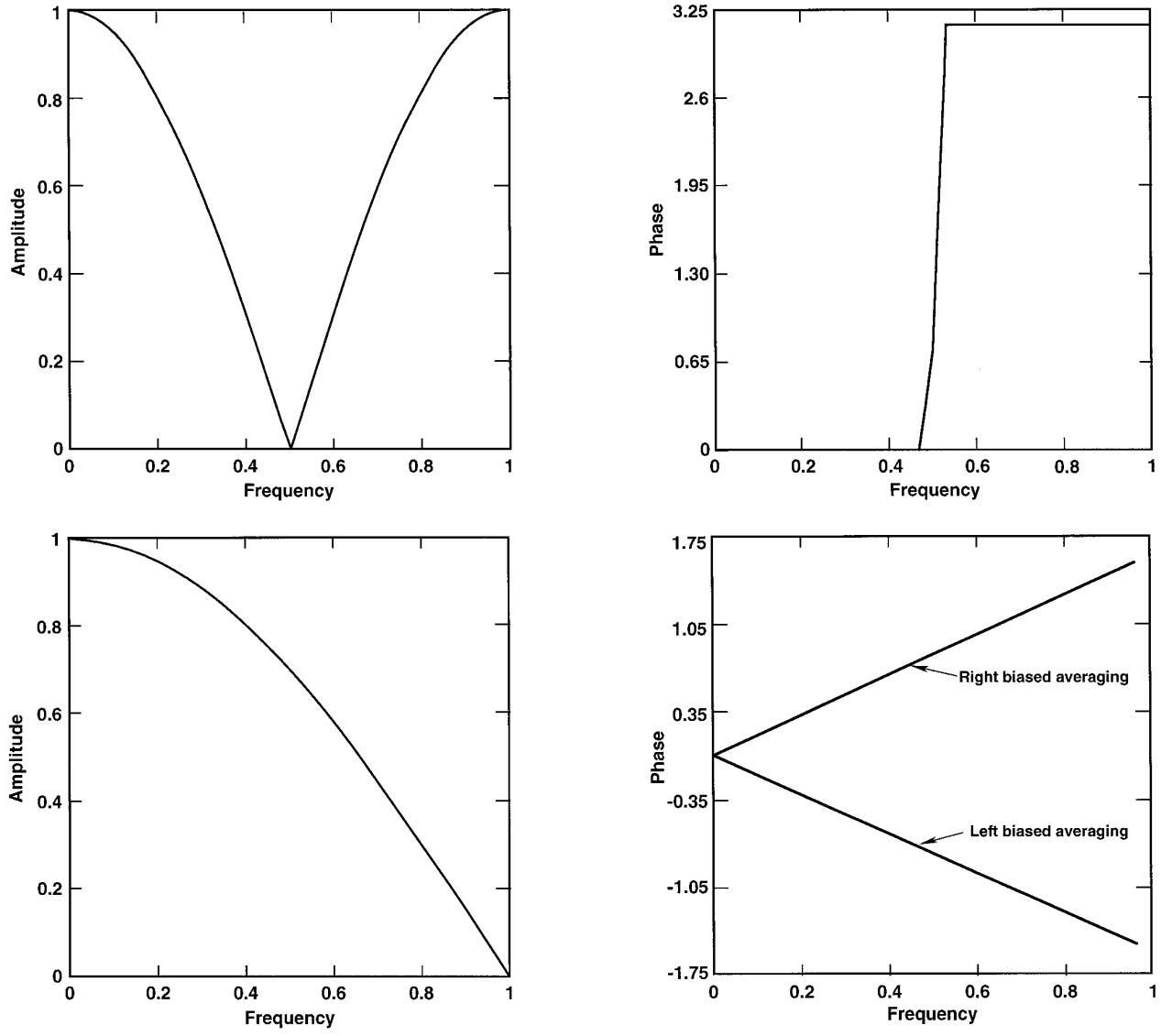

FIG. 8. (a) Frequency domain of unbiased averaging operator (amplitude); (b) frequency domain of unbiased averaging operator (phase). (c) frequency domain of biased averaging operator (amplitude); (d) Frequency domain of biased averaging operator (phase).

location j by a time step Δt, we draw a characteristic line with slope $\Delta t/\Delta x = -1/\mathbf{a}$ and locate the intersection point of this line with the spatial coordinate at time t, which is $-\mathbf{a}\,\Delta t$ from location j. Then

$$U_j^{n+1} = U_j + \left[\frac{U_j - U_{j-1}}{x_j - x_{j-1}}\right](-\mathbf{a}\,\Delta t)$$

$$U_j^{n+1} = U_j - \lambda(U_j - U_{j-1}),$$

where Δx is used to represent the mesh spacing given by $x_j - x_{j-1}$. This step is the map back to the discrete set at time level $n + 1$. This difference scheme can be obtained with a first-order accurate upwind differencing for U_x at location j and using a forward Euler time integration to update the solution at location j to the new time level.

The response function for this scheme is a delta function located at $j = 1$ and another located at $j = 2$. The multiplication factors are $(1 - \lambda)$ and λ at $j = 1$ and $j = 2$, respectively. A fully upwind scheme is a causal response function. Matrix representation for this scheme is lower triangular Toeplitz. Eigenvalue in the frequency domain is

$$1 - \lambda + \lambda\cos(2\pi f\,\Delta x) - i\,\lambda\sin(2\pi f\,\Delta x).$$

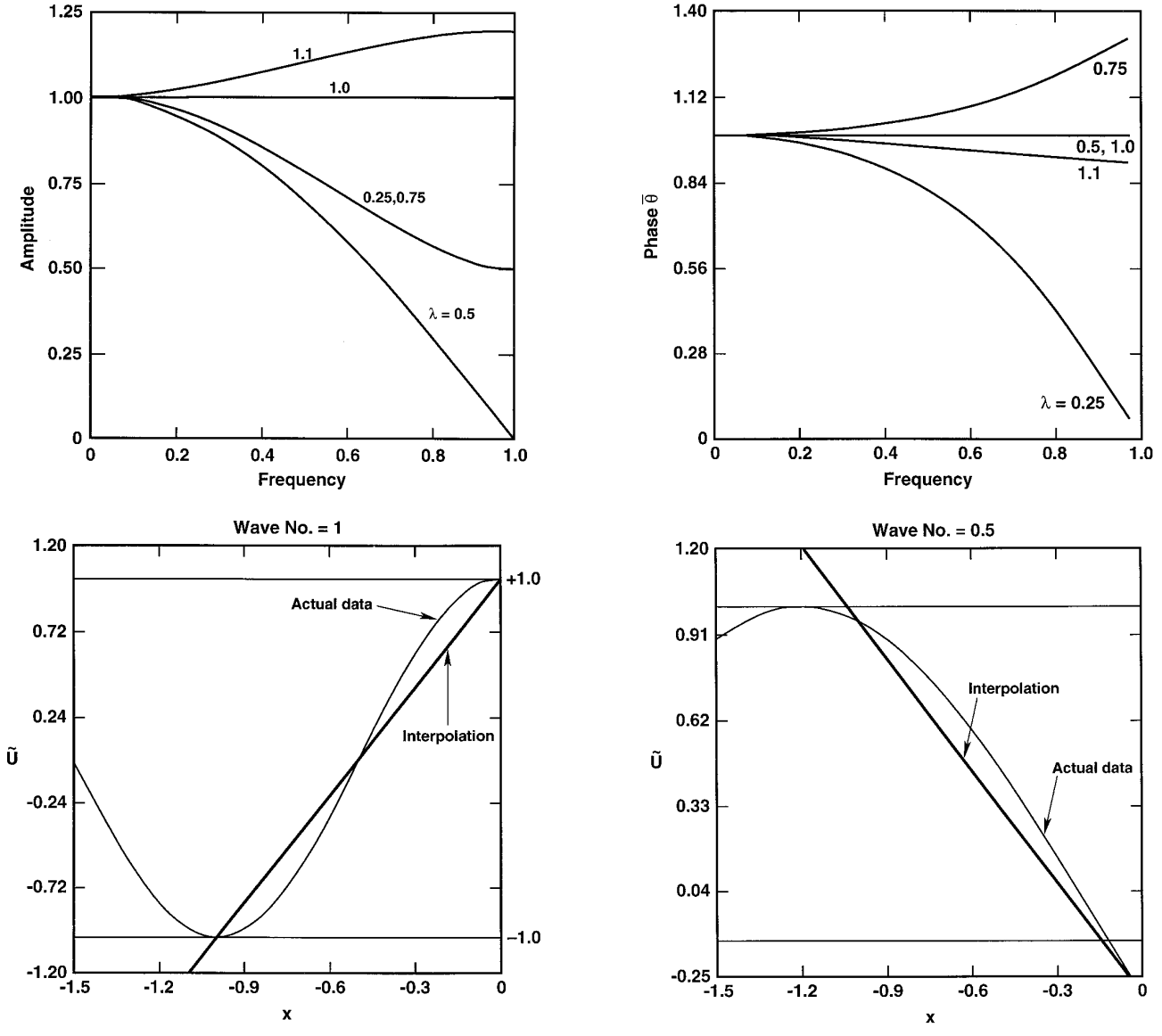

FIG. 9. Frequency and physical domains of first-order upwind scheme: (a) amplitude response; (b) phase response; (c) wave no. = 1.0; (d) wave no. = 0.5.

Spectral characteristics of this operator are shown in Figs. 9a and 9b. For pure advection the phase variation is from $-\pi\lambda$ to $+\pi\lambda$ in the frequency range $-f_n$ to $+f_n$. Phase lead or lag is determined by

$$\bar{\theta} = \frac{\text{phase of response at frequency } f}{\text{phase for pure advection at } f}.$$

If the value of $\bar{\theta}$ is greater than one, the phase of the response function leads the phase for pure advection at that wave number. The numerical scheme will advect a signal with speed less than **a** at all wave numbers where $\bar{\theta}$ is less than 1.

For the first-order upwind scheme, amplification is less than or equal to one at all frequencies for $\lambda \leq 1$, with the higher wave numbers suffering the most damping. Phase errors are also higher at these wave numbers. Figure 9b shows the variation of $\bar{\theta}$. At λ of 0.75, $\bar{\theta}$ is > 1 at almost all wave numbers, which means that the numerical solution leads the exact solution (propagates with higher speed than **a**). Operating with λ less than one also implies that only interpolated values for $\tilde{U}$ are used, with $\tilde{U}$ varying in a linear fashion between x_{j-1} and x_j. Since the interpolation is linear, values generated in the continuous space is bounded by U_j and U_{j-1} for all $x_{j-1} \leq x \leq x_j$. When λ exceeds unity, the value used to update U_j^{n+1} is an extrapo-

lation from the linear fit between U_{j-1} and U_j. Figures 9c and 9d show the interpolated and actual data in the physical domain for wave numbers 1 and 0.5. In both cases the interpolated value crosses the bounds ± 1.0 at $x < -1.0$. Choosing the value from $x = -1.0$ to update the value at j is equivalent to integrating with $\lambda = 1.0$. Amplification in the spectral domain corresponds to the generation of new maxima or minima by the choice of interpolation in the physical domain.

At $\lambda = 0.5$ and $\lambda = 1.0$ this scheme is symmetric about $j = \frac{1}{2}$ and $j = 1$, respectively. Schemes that display such symmetry can be shown to have minimum distortion or the perfect shift property at these values for λ. Figure 9b shows zero phase error at $\lambda = 0.5$ and $\lambda = 1.0$. For $\lambda = 0.5$, eigenvalue of this scheme is

$$e^{-i2\pi f \Delta x/2} \cos(\pi f \Delta x),$$

whose phase shift is exact but the higher frequencies are attenuated. If the input signal were band-limited, operating this scheme at λ will not result in appreciable loss in the signal strength. At $\lambda = 1.0$, the eigenvalue in the frequency domain is $e^{-i2\pi f \Delta x}$ resulting in no phase or amplitude errors over the entire frequency spectrum. U^{n+1} is obtained by simply shifting the elements of U^n to the right by one at every time step.

THE LAX–WENDROFF SCHEME

Fitting a parabola between $j - 1 (x = -\Delta x)$, j, and $j + 1 (x = +\Delta x)$ for $\tilde{U}(x)$ results in

$$\tilde{U}(x) = U_j + \left[\frac{U_{j+1} - U_{j-1}}{2\,\Delta x}\right] x + \left[\frac{U_{j+1} - 2U_j + U_{j-1}}{\Delta x^2}\right] \frac{x^2}{2}.$$

For advection with $a > 0$, the updated value at location j is obtained from the spatial location $x = -\mathbf{a}\,\Delta t$. The Lax–Wendroff scheme is formally second-order accurate. This operator is no longer causal. Frequency domain representation has the eigenvalues

$$1 + \lambda^2(\cos(2\pi f \Delta x) - 1) - i\lambda \sin(2\pi f \Delta x).$$

The spectral characteristics for this scheme are given in Figs. 10a and b. Amplification is less than unity at all wave numbers for $\lambda < 1$. At $\lambda = 0.25$, damping at a higher frequency is smaller than that at $\lambda = 0.5$ and 0.75. The numerical solution has a large phase lag at $\lambda = 0.25$ and 0.5 at the higher frequencies. At $\lambda = 0.75$ high wave numbers have a phase lead, as well as more severe damping. This scheme has a perfect shift at λ of 1 and -1. Figures 10c and 10d show the interpolated and the actual data for this scheme in the physical domain at wave numbers 1.0 and 0.5, respectively. The interpolated value crosses the lower (-1.0) or the upper bound $(+1.0)$ at $x = -1.0$. Using a $\lambda > 1.0$ to update the value at j will generate a new global maxima or a minima for almost all wave numbers. In the physical domain interpolated value at $x = -1.05$ is -1.2 for input at the Nyquist frequency which is the amplification obtained in the spectral domain for this wave number at $\lambda = 1.05$. For all $\lambda \leq 1$, amplification at all frequencies that can be captured on the grid is ≤ 1, making the scheme conditionally stable.

THE THREE-POINT UPWIND SCHEME

If we restrict the interpolation domain to remain one-sided, ranging from $j - 2$ to j and fit a parabola,

$$\tilde{U}(x) = U_j + \left[\frac{3U_j - 4U_{j-1} + U_{j-2}}{2\,\Delta x}\right] x + \left[\frac{U_j - 2U_{j-1} + U_{j-2}}{\Delta x^2}\right] \frac{x^2}{2}.$$

The linear term is a second-order accurate representation of the first derivative at j, and the coefficient of the quadratic term is the second derivative at $j - 1$. To update the solution at j, we substitute $x = -\mathbf{a}\,\Delta t$ in the above equation. This scheme is second-order accurate and can operate in a stable fashion up to a λ of 2. It has a perfect shift at $\lambda = 1$ and $\lambda = 2$.

The spectral characteristics are shown in Figs. 11a and 11b. The eigenvalue for this operator in the frequency domain is

$$\begin{aligned} &1 - 1.5\lambda + 0.5\lambda^2 + (2\lambda - \lambda^2)\cos(2\pi f \Delta x) \\ &\quad + (-0.5\lambda + 0.5\lambda^2)\cos(4\pi f \Delta x) \\ &\quad + i[(-2\lambda + \lambda^2)\sin(2\pi f \Delta x) \\ &\quad + (0.5\lambda - 0.5\lambda^2)\sin(4\pi f \Delta x)]. \end{aligned}$$

In the stable range of operation, all values of λ (except 1.0 and 2.0) damp the high frequency waves. Phase errors are larger at smaller λ. Although the phase error is relatively small for $\lambda = 1.75$, the amplitude damping is severe at higher frequencies. Figure 11c shows the interpolation in the physical domain for a wave number of 1.0. In Fig. 11d we see the result of interpolation for data at a wave number of 0.5. In both these cases, new global maxima or minima are generated in the physical domain when λ exceeds 2.0. Although $\lambda = 2.1$ generates large amplification at the high frequencies, signals with a wave number of up to 0.2 are not amplified (Fig. 11a). Interpolation for this wave number in the physical domain is shown in Fig. 11e.

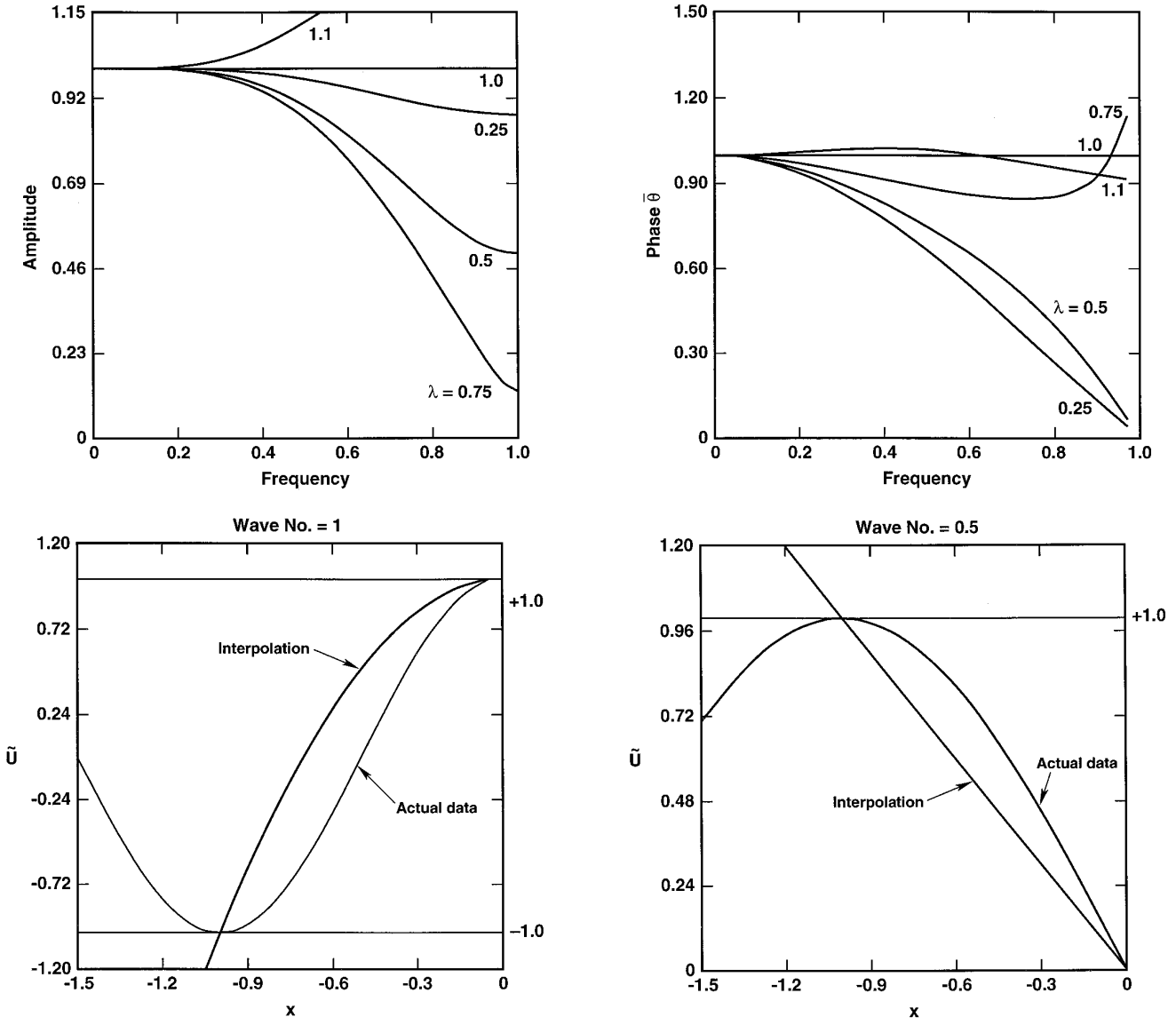

FIG. 10. Frequency and physical domains of Lax–Wendroff scheme: (a) amplitude response; (b) phase response; (c) wave no. = 1.0; (d) wave no. = 0.5.

Only when the choice of the location from where the value for $\tilde{U}$ is chosen to update the value at j exceeds -2.25 (equivalent to a $\lambda > 2.25$) are new maxima generated for data at a wave number of 0.2.

Instead, if a three-point stencil from $j-2$ to j is used for approximating U_x and the forward Euler is used for time integration, the resulting scheme is unstable at almost all values of λ. The perfect shift property is also lost. In this case U_j at time level $n+1$ is given by

$$U_j^{n+1} = U_j - \lambda\left[\frac{3U_j - 4U_{j-1} + U_{j-2}}{2}\right]$$

whose eigenvalue in the frequency domain is

$$1 - 1.5\lambda + 2\lambda\cos(2\pi f\Delta x) - 0.5\lambda\cos(4\pi f\Delta x) + i[-2\lambda\sin(2\pi f\Delta x) + 0.5\lambda\sin(4\pi f\Delta x)].$$

In the physical domain, this scheme is obtained from the cubic fit used in the previous example by neglecting the quadratic term. Slope at point j is obtained from the slope of a cubic passing through U at $j-2$ through j, and a linear variation is assumed for $\tilde{U}$ along this slope. This scheme is first-order accurate and has an amplification factor greater than one for some wavelengths at all but the smallest λ (Fig. 12a), but the higher wave numbers are not affected at λ smaller than 0.5. The phase either lags or leads (Fig. 12b) at all but the smallest wave numbers, regardless of the value of λ used

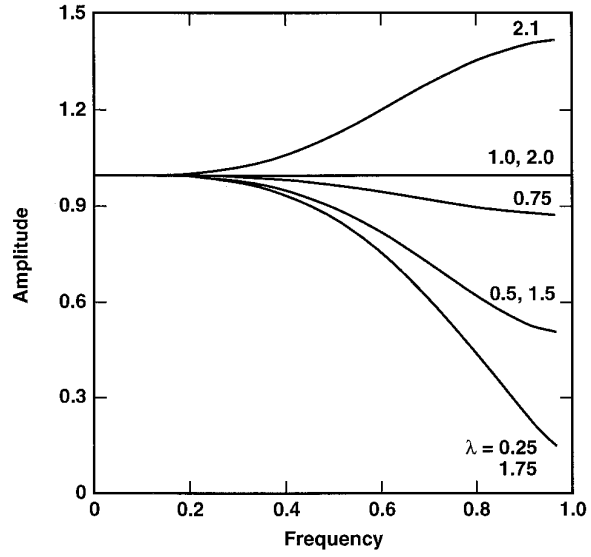

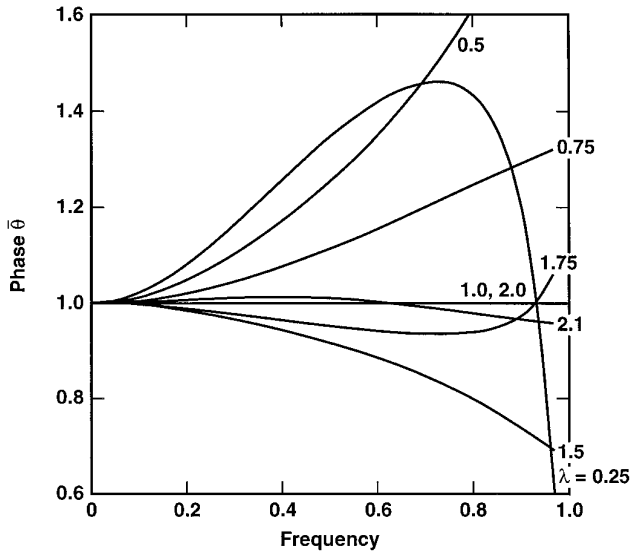

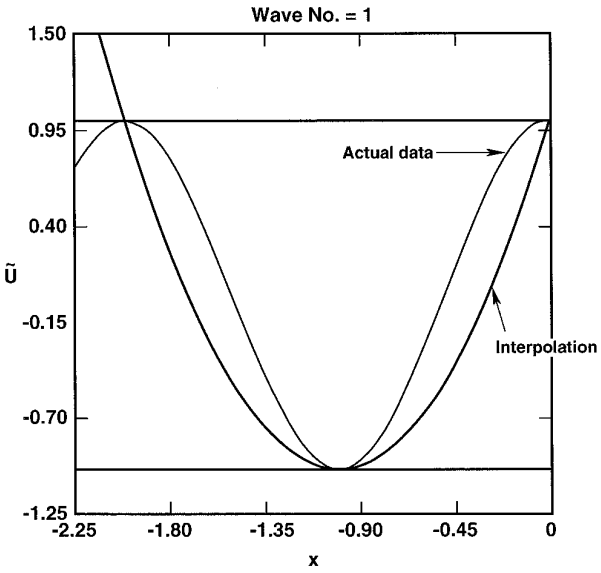

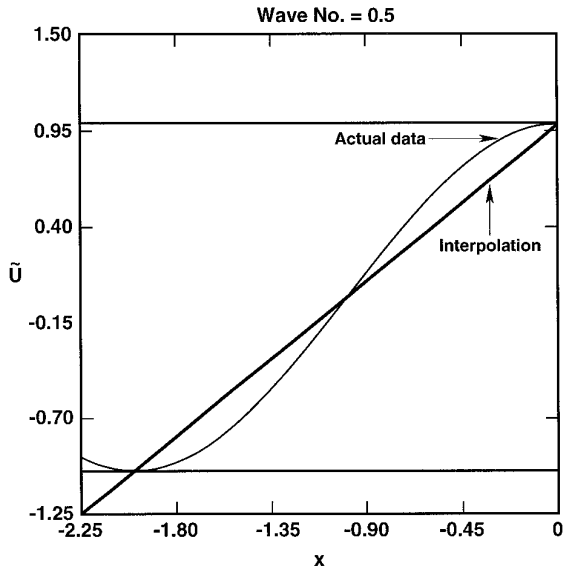

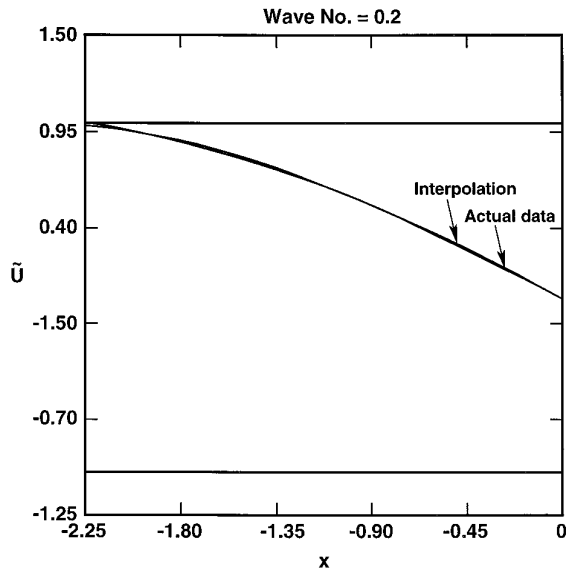

FIG. 11. Frequency and physical domains of scheme based on quadratic fit: (a) amplitude response; (b) phase response; (c) wave no. = 1.0; (d) wave no. = 0.5; (e) wave no. = 0.2.

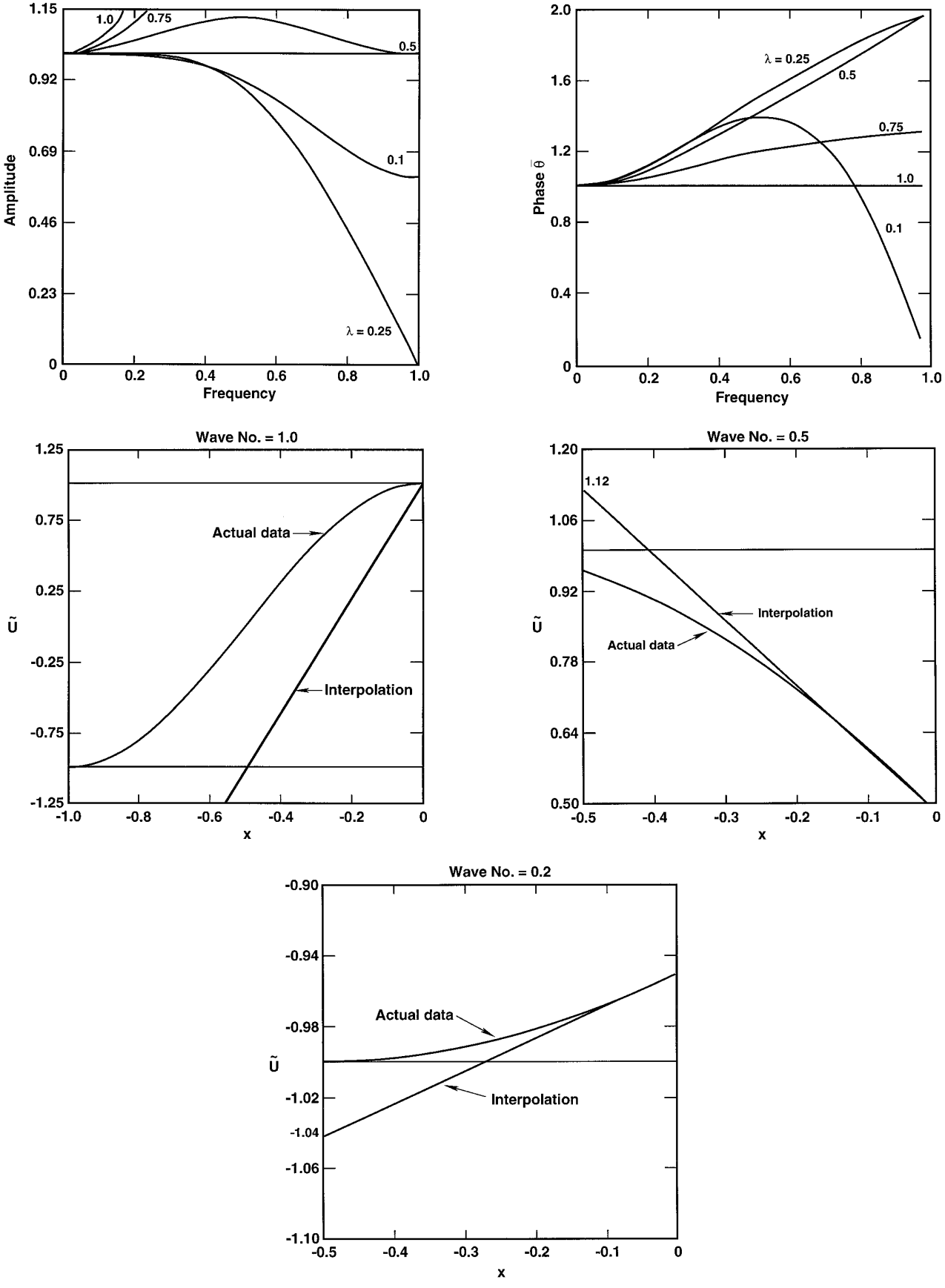

FIG. 12. Frequency and physical domains of scheme based on three-point fit for u_x: (a) amplitude; (b) phase response; (c) wave no. = 1.0; (d) wave no. = 0.5; (e) wave no. = 0.2.

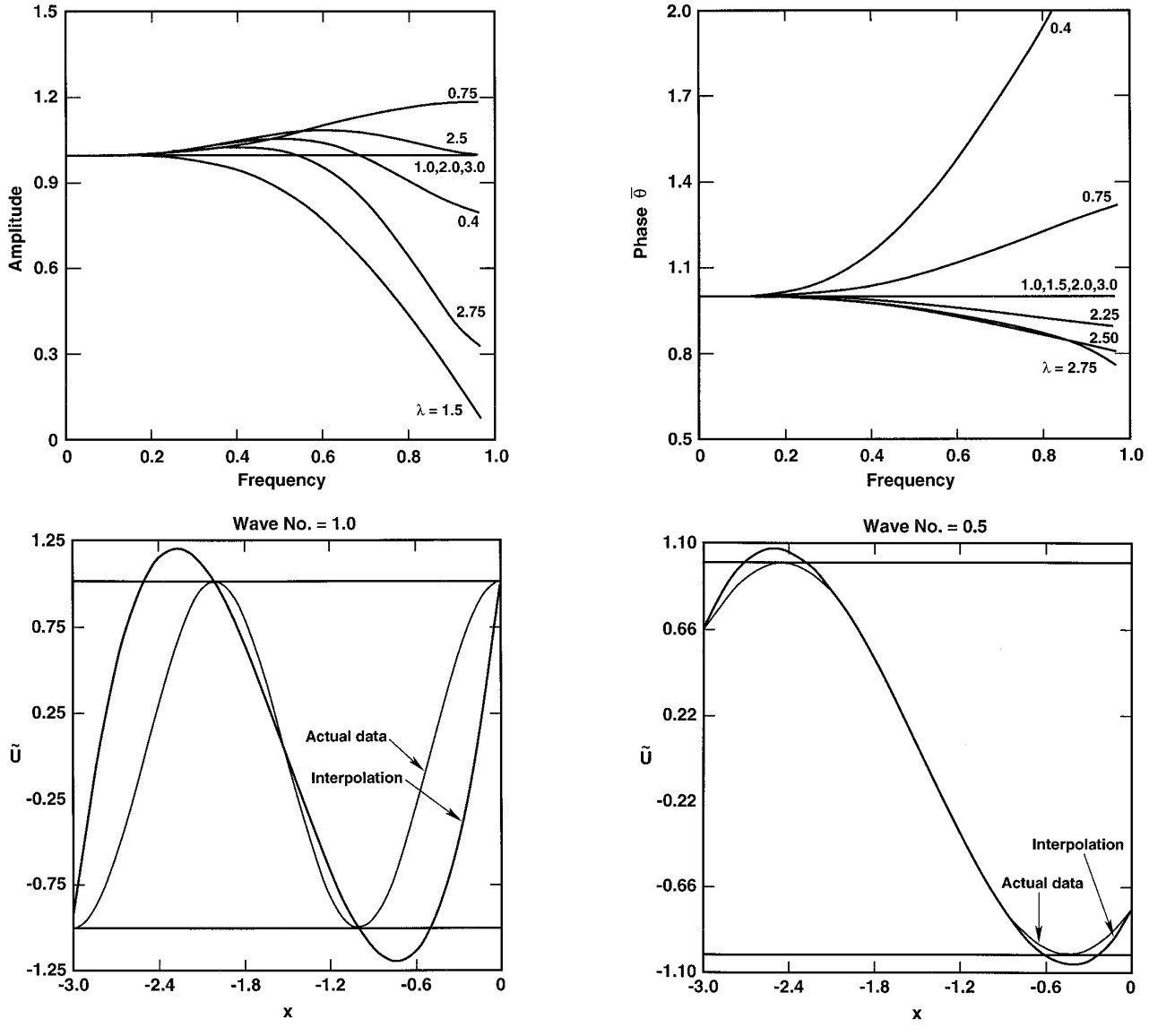

FIG. 13. Frequency and physical domains of scheme based on cubic fit: (a) amplitude response; (b) phase response; (c) wave no. = 1.0; (d) wave no. = 0.5.

in the integration. Figures 12c–e show the interpolation in the physical domain. Amplification for the highest wave number in the frequency domain (Fig. 12a) is 1 for $\lambda = 0.5$ and is verified by Fig. 12c, showing the interpolation in the physical domain. At $x = -0.5$ ($\lambda = 0.5$), the interpolated curve crosses the lower bound -1.0 and for all $\lambda > 0.5$, new minima arise. Figure 12d shows the interpolated value generating a maxima (1.12) at a spatial location of -0.5 for a wave number equal to a half. The amplification for $\lambda = 0.5$ in the spectral domain for wave number 0.5 is also 1.12. At a lower frequency, a wave number $=0.2$, minimum in the physical domain (Fig. 12e) is -1.04. The amplification from the frequency domain at $\lambda = 0.5$ is also 1.04 at this wave number. This scheme is not suitable for advection equations.

THE FOUR-POINT UPWIND SCHEME

Increasing the degree of the polynomial to 3 results in a cubic fit from $j - 3$ to j:

$$\tilde{U}(x) = U_j + \left[\frac{U_j - 3U_{j-1} + 3U_{j-2} - U_{j-3}}{\Delta x^3}\right]\frac{x^3}{6} + \left[\frac{2U_j - 5U_{j-1} + 4U_{j-2} - U_{j-3}}{\Delta x^2}\right]\frac{x^2}{2} + \left[\frac{11U_j - 18U_{j-1} + 9U_{j-2} - 2U_{j-3}}{6\Delta x}\right]x.$$

Integration of the advection equation is accomplished

by replacing x by $-\mathbf{a} * \Delta t$. This scheme is stable for $1 \leq \lambda \leq 2$ and is third-order accurate. In this range, the amplification does not exceed 1 at all wave numbers, but the scheme can have growing modes for λ in the range 0 to 1 as well as above 2 (Figs. 13a and 13b). In the stable range, $\lambda = 1.5$ has good phase characteristics (no lag or lead over the entire spectrum), but the damping at high wave numbers is large. The eigenvalue of this scheme is

$$
\begin{aligned}
&1 - \tfrac{11}{6}\lambda + \lambda^2 - \tfrac{1}{6}\lambda^3 \\
&\quad + (3\lambda - 2.5\lambda^2 + 0.5\lambda^3)(\cos(2\pi f\,\Delta x) - i\sin(2\pi f\,\Delta x)) \\
&\quad + (-1.5\lambda + 2\lambda^2 - 0.5\lambda^3)(\cos(4\pi \mathrm{f}\,\Delta x) - i\sin(4\pi f\,\Delta x)) \\
&\quad + (\tfrac{1}{3}\lambda - 0.5\lambda^2 + \tfrac{1}{6}\lambda^3)(\cos(6\pi f\,\Delta x) - i\sin(6\pi f\,\Delta x)).
\end{aligned}
$$

Next we look at the interpolation in the physical domain using the third-order polynomial given above. For data at the Nyquist frequency (Fig. 13c) interpolation shows a lower minima, -1.1875, at a x location of $x = -0.75$. The original data is a sine wave at the Nyquist frequency, with a phase shift of $\pi/2$. In the frequency domain (Fig. 13a) the operator gives the same amplification 1.1875 for the Nyquist frequency at $\lambda = 0.75$. At a wave number of 0.5, the interpolated value has a new minima 1.053 (Fig. 13d) at $x = -0.4$, which is about the same magnification (1.057) in the spectral domain at one-half of the Nyquist frequency for $\lambda = 0.4$.

CONCLUSIONS

We have presented the stability characteristics of a few numerical schemes, used in integrating advection equations, in both frequency and physical domains. By treating the integration for the advection equation as a convolution of a response function with the data at time $t = 0$, we have used FFT to obtain both phase and amplitude variation over the entire frequency range. Examples presented here show that updating the solution at a spatial location is equivalent to choosing a value from the interpolated value at the previous time level and that the location from where the interpolated value is chosen is determined by λ. We have shown that, when the amplification factor for certain wave numbers at a fixed λ is greater than one in the frequency domain, a corresponding extremum occurs in the physical domain at that spatial location for input at that frequency. The location at which the interpolation crosses the bounds at time level n determines the boundary of a stable operation. The absolute value of this extrema in the physical domain matches the amplification factor from the frequency domain.

For a numerical scheme for the advection equation to be stable, the choice of interpolation is critical. It determines the stability bounds within which an explicit numerical scheme can safely integrate the equation. Smart interpolation schemes that do not generate extrema should therefore lead to more stable explicit schemes. The interpolation has to meet this criterion over all frequency ranges that can be captured on the grid. TVD [7] and ENO [8] schemes meet this criterion. The spectral characteristics of implicit schemes will be presented in a separate paper.

REFERENCES

1. R. D. Richtmyer and K. W. Morton, *Difference Methods for Initial-Value Problems* (Interscience, New York, 1967).
2. C. Hirsch, *Numerical Computation of Internal and External Flows. Vol. 1. Fundamentals of Numerical Discretization* (Wiley, New York, 1989).
3. B. N. Parlett, *The Symmetric Eigenvalue Problem*, Comput. Math. Ser. (Prentice–Hall, Englewood Cliffs, NJ, 1980).
4. G. Strang, *Linear Algebra and its Applications* (Academic Press, New York/London, 1980).
5. G. M. Jenkins and D. G. Watts, *Spectral Analysis and its Applications*, Series in Time Series Analysis (Holden–Day, Oakland, CA, 1968).
6. S. L. Marple Jr., *Digital Spectral Analysis with Applications*, Signal Processing Series (Prentice–Hall, Englewood Cliffs, NJ, 1987).
7. S. R. Chakravarthy and S. Osher, AIAA Paper No. 85-0363 (unpublished).
8. A. Harten and S. R. Chakravarthy, UCLA Computational and Applied Mathematics (CAM) Report 91-16, September 1991; also ICASE Report 91-76, September 1991 (unpublished).